Rapid report

Methanogenic Archaea dominate mature heartwood habitats of Eastern Cottonwood (*Populus deltoides*)

Author for correspondence:
Christopher W. Schadt
Tel: +1 865 576 3982
Email: schadtcw@ornl.gov

Received: *18 April 2018*
Accepted: *14 June 2018*

Daniel Z. Yip[1]*, Allison M. Veach[1]*, Zamin K. Yang[1], Melissa A. Cregger[1,2] and Christopher W. Schadt[1,3]*

[1]Biosciences Division, Oak Ridge National Laboratory, Oak Ridge, TN 37831, USA; [2]Department of Ecology and Evolutionary Biology, University of Tennessee, Knoxville, TN 37996, USA; [3]Department of Microbiology, University of Tennessee, Knoxville, TN 37996, USA

Summary

- While recent reports demonstrate that the direct emission of methane from living tree trunks may be a significant terrestrial emission source, there has been debate whether tree emissions are due to transport from soils or produced in the wood environment itself. Reports of methanogens from wood of trees were prominent in the literature 40 years ago but have not been revisited with molecular ecology approaches.
- We examined communities associated with *Populus deltoides* using rRNA gene sequence analyses and how these vary with tree and wood properties.
- Our data indicate that wood environments are dominated by anaerobic microbiomes. Methanogens are prominent in heartwood (mean 34% relative abundance) compared to sapwood environments (13%), and dominant operational taxonomic units (OTUs) were classified as the *Methanobacterium* sp. Members of the Firmicutes phylum comprised 39% of total sequences and were in 42% greater abundance in sapwood over heartwood niches. Tree diameter was the strongest predictor of methanogen abundance, but wood moisture content and pH were also significant predictors of taxon abundance and overall community composition.
- Unlike microbiomes of the soil, rhizosphere and phyllosphere, wood associated communities are shaped by unique environmental conditions and may be prominent and overlooked sources of methane emissions in temperate forest systems.

Introduction

Methane is an impactful greenhouse gas accounting for 20% of radiative forcing since 1750 (Saunois *et al.*, 2016). Modeling approaches incorporating biogenic, thermogenic, and pyrogenic methane emissions have been unable to accurately quantify global methane budgets (Saunois *et al.*, 2016). Recently, several reports from diverse forest types and tree species have demonstrated that the direct emission from living tree trunks may be a significant source of terrestrial methane emissions (Covey *et al.*, 2012; Pangala *et al.*, 2014, 2015; Machacova *et al.*, 2016; Wang *et al.*, 2016; Pitz & Megonigal, 2017; Warner *et al.*, 2017; Maier *et al.*, 2018; Pitz *et al.*, 2018). In some cases, the magnitude of this source may be equal to or greater than the methane sink in upland forest soils

(Covey *et al.*, 2012; Pitz & Megonigal, 2017) and potentially account for the gap in tropical forest methane budgets (Pangala *et al.*, 2017). Despite this, evidence is mixed as to whether methane is produced within trees or whether trees (Covey *et al.*, 2012; Wang *et al.*, 2016) just act as conduits for methane gas produced and transported from the subsurface (Pangala *et al.*, 2013, 2017). Indeed, both mechanisms may be important depending on tree species (e.g. those containing dry and dense vs wet and porous wood) and ecosystem under study (e.g. wetland vs upland forest soils).

Microbiological investigations of living wood have been conducted in the past (Zeikus & Ward, 1974; Zeikus & Henning, 1975; Ward & Zeikus, 1980; Schink *et al.*, 1981a,b, 1982), but these studies primarily focused on *ex situ* wood incubations and the isolation of microbial representatives, rather than overall community characterization across tree conditions. For example, Zeikus &

*These authors contributed equally to this work.

Ward (1974) demonstrated that methane production occurred from extracted wood tissue from *Populus deltoides* and were able to isolate pure cultures of a new species, *Methanobacterium arborphilicum* (Zeikus & Henning, 1975), later reclassified as *Methanobrevibacter arboriphilus* (Balch *et al.*, 1979). *Methanobrevibacter arboriphilus* has become a well-studied model organism due to its' tolerance and growth in the presence of low levels of oxygen through detoxification by a $F_{420}H_2$ oxidase (Kiener & Leisinger, 1983; Seedorf *et al.*, 2004, 2007; Tholen *et al.*, 2007). To our knowledge, this isolate remains the only cultured representative of wood inhabiting methanogens. Other wood associated microbial groups that have been isolated include *Clostridium*, *Bacteroides*, *Klebsiella*, *Erwinia*, *Herbaspirillum*, *Acinetobacter*, *Enterobacter* and *Burkholdaria*, many of which have been isolated from woody tissues; and may be anaerobic, fermentative, carry out acetylene reduction, or contain nitrogenase genes for nitrogen fixation (Schink *et al.*, 1981a,b, 1982; Warshaw *et al.*, 1985; Streichan & Schink, 1986; Doty *et al.*, 2005, 2009; Xin *et al.*, 2009).

Our study goal was to identify the bacterial and archaeal microbiome associated with the wood of mature, living, Eastern Cottonwood (*Populus deltoides*) trees and test for relationships between microbial community composition, assessed using molecular ecology tools, and tree/wood properties. Based upon past work and our own informal observations of odors associated with tree coring at these sites indicative of fermentative environments, we hypothesized that an anaerobic community including methanogenic archaea would dominate woody tissue, particularly in heartwood tissue which is often water-soaked. We hypothesized that tree diameter, wood pH, and wood moisture content would correlate with microbiome composition and methanogen abundance, as these could influence anaerobic conditions and microbial growth in the woody tissue environment.

Materials and Methods

Populus wood tissue sampling and analysis

Wood samples were collected from *Populus deltoides* at four study locations along the Caney Fork River in East Tennessee (Table 1). The characteristics of these sites were reported in previous studies (Gottel *et al.*, 2011; Shakya *et al.*, 2013) and the subset of sites studied here included some of the same trees. A random selection of 13 living trees ($n = 3$ per site, except site 1 which had $n = 4$) at least 35 cm diameter at breast height (DBH), were sampled on June 29, 2016. Sampled trees were randomly selected from living trees with no signs of butt rot, hollowing, or other damage. Two cores were taken for each tree at perpendicular angles and cored into the pith at *c.* 1 m in height and used as sub-replicates throughout the study. The increment borer was sanitized with ethanol between samples. Each core was split into sapwood and heartwood based on depth and coloration and stored in separate 15 ml conical tubes. Sapwood was typically *c.* 12 cm in depth not including bark, the remainder of the core being heartwood. Samples were kept on ice until returning to the laboratory where they were stored at $-80°C$. After extraction of each core from the increment borer, a lighter was used to spot check for the presence of flammable gasses (Fig. 1; Supporting Information Videos S1–S4). A subsample of roughly chopped wood was used for moisture content determination by drying at $70°C$ to a constant mass. Dried samples were weighed and ground to a fine powder for pH determination. Approximately 150 µl of wood powder was mixed with 1.2 ml of sterile water and incubated on a plate shaker (600 rpm) for 1 h. Samples were centrifuged at 13 000 *g* for 2 min and the supernatant was measured for pH. Due to limited material, wood pH was only measured for heartwood tissues, whereas moisture content was measured for both tissue types.

DNA extraction and Illumina MiSeq sequencing

Heartwood and sapwood subsamples were finely minced (< 2 mm). DNA was extracted from replicate cores ($n = 2$ per tree) using the MoBio PowerPlant kit (MoBio, Carlsbad, CA, USA), with the following modifications. The supplied beads were replaced with a single 6.35 mm steel ball bearing added to each tube with 50 mg of minced tissue. Tubes were then frozen in liquid nitrogen and the material ground at 30 Hz for 60 s in a Restch MM400. Freezing and grinding were repeated for two additional cycles. Six technical replicates of each sample were extracted and then combined to increase DNA yields. To remove PCR inhibitors, DNA samples were further processed using the MoBio PowerClean kit as described by the manufacturer. DNA was quantified in a Nanodrop 1000 spectrophotometer (Wilmington, DE, USA) and confirmed by Qubit 2.0 fluorometry (Invitrogen, Carlsbad, CA, USA). We used a two-step PCR approach for 16S rRNA gene amplification and DNA sequencing developed previously (Lundberg *et al.*, 2013) with several modifications to included primers and procedures as described previously (Cregger *et al.*, 2018).

Bioinformatics and statistical analysis

Forward and reverse primers and sequencing adapters were removed using the program cutadapt (Martin, 2011). All additional analyses were done within QIIME (Caporaso *et al.*, 2010) using the quality control parameters and procedures described previously (Cregger *et al.*, 2018) except CHIMERA SLAYER was used for chimeric sequence detection (Haas *et al.*, 2011). Samples were rarefied to 7900 sequences per sample, which yielded adequate sequencing coverage based on rarefaction curves (Fig. S1) and Good's coverage estimates. The final, rarefied dataset contained 426 600 sequences representing 3597 operational taxonomic units (OTUs). Diversity indices were calculated in QIIME – OTU richness (S_{obs}), the complement of Simpson's diversity ($1 - D$), Simpson's evenness (E), and Faith's phylogenetic diversity (PD) on the rarefied dataset. The Phylogenetic Investigation of Communities by Reconstruction of Unobserved States (PICRUSt) pipeline was performed (Langille *et al.*, 2013) to predict metagenome functional content from the 16S rRNA gene data. Briefly, data were normalized by copy number, a virtual metagenome of KEGG ortholog abundances was predicted for each sample in the OTU table, and the results were categorized by function. KEGG maps for methane metabolism and nitrogen

Table 1 Caney Fork River riparian study locations and *Populus deltoides* tissue descriptions

Study location	Tissue type	GPS coordinates	OTU richness[a]	Simpson's diversity	Simpson's evenness	Faith's PD[a]
S1	Heartwood	36°08′32.4″N 85°48′24.0″W	212 ± 24	0.82 ± 0.02	0.03 ± 0.003	13.2 ± 1.4
S1	Sapwood		390 ± 128	0.86 ± 0.06	0.06 ± 0.02	18.9 ± 4.7
S2	Heartwood	36°06′02.4″N 85°49′48.2″W	222 ± 49	0.86 ± 0.02	0.04 ± 0.01	13.1 ± 2.5
S2	Sapwood		434 ± 156	0.89 ± 0.04	0.07 ± 0.02	21.7 ± 4.9
S3	Heartwood	36°08′45.2″N 85°51′53.0″W	247 ± 24	0.89 ± 0.03	0.05 ± 0.01	15.1 ± 0.6
S3	Sapwood		409 ± 81	0.90 ± 0.03	0.06 ± 0.02	23.6 ± 3.4
S4	Heartwood	36°13′26.7″N 85°54′39.5″W	237 ± 20	0.91 ± 0.01	0.05 ± 0.01	14.3 ± 0.9
S4	Sapwood		271 ± 39	0.81 ± 0.13	0.05 ± 0.02	17.3 ± 2.1

The mean and standard error are given for all microbial diversity estimates. Operational taxonomic unit (OTU) richness and Faith's phylogenetic diversity (PD) were significantly greater in sapwood tissue compared to heartwood (ANOVA, $P \leq 0.02$). [a]Denotes a diversity metric that differed between tissue type.

Fig. 1 An example of flammable gasses being emitted from increment borers inserted in *Populus deltoides* trees just after sampling (see Supporting Information Videos S1–S4 for other observations).

metabolism were colored by the abundance of KEGG orthologs using the KEGG Mapper Color Pathway analysis tool. Predicted mcrA gene abundances were then determined for the heartwood and sapwood samples.

Two-way analysis of variance (ANOVA) models were used to determine if microbial diversity and dominant bacterial and archaeal phyla (subphyla for Proteobacteria) differed across study locations and tissue type (heartwood vs sapwood). Stepwise multiple regression modeling using an Akaike information criterion (AIC) minimization procedure was used to determine which tree physical measurement correlated most strongly with diversity and dominant phyla/subphyla within heartwood and sapwood tissues. These models were run separately for each tissue type and data from the two sub-replicate cores from each tree averaged before analyses. Both Bray–Curtis and Unifrac dissimilarity (weighted, unweighted (Lozupone *et al.*, 2006)) were calculated via QIIME and visualized using principal coordinates analysis (PCoA). Dissimilarity metrics were used as input for adonis analysis, a permutational multivariate analysis of variance (perMANOVA) test (Anderson, 2001), to detect the amount of variation explained by study location and tissue type for both taxonomic and phylogenetic beta diversity. Lastly, we used SIMPER analysis to determine which OTUs contributed significantly to differences between tissue types. We report only those that are dominant OTUs ($\geq 0.1\%$ mean relative abundance across all samples) although a list of all SIMPER

detected OTUs are provided (Table S1). After testing for equal variance, a Student's *t*-test was also performed to determine if predicted mcrA abundance differed between sapwood and heartwood samples. Statistical analyses were done in R v.3.3.2 using the VEGAN (Oksanen *et al.*, 2015) and LABDSV (Roberts, 2016) packages. Sequence data are available through the National Center for Biotechnology Information (Bioproject accession PRJNA450753).

Results

Microbial diversity

Taxonomic OTU richness ($F_{1,25} = 6.79$, $P = 0.02$) and Faith's PD differed significantly between tissue type ($F_{1,25} = 9.25$, $P = 0.006$) and were greater in sapwood tissue compared to heartwood (Table 1). Specifically, sapwood had 49% greater number of OTUs (378 ± 53) and 38% greater phylogenetic diversity (20.3 ± 1.9) compared to heartwood tissue (228 ± 14 OTUs; 13.9 ± 0.7 Faith's PD). Study site location did not influence these estimates ($P \geq 0.65$). Simpson's diversity and evenness did not differ across study location or tissue type ($P \geq 0.14$). Only evenness within heartwood correlated moderately with any tree physical measurement (Full model: Adj. $R^2 = 0.30$, $F_{2,10} = 3.52$, $P = 0.07$). Evenness correlated positively with tree DBH in heartwood tissues ($T = 2.62$, $P = 0.03$).

Microbial taxon abundances and community composition

The most dominant phyla ($> 1\%$ relative abundance) were Firmicutes (39.2%), Euryarchaeota (23.9%), Bacteroidetes (9.3%), Actinobacteria (8.8%), Spirochaetes (5.7%), Deltaproteobacteria (4.3%), Alphaproteobacteria (2.3%), Chloroflexi (1.3%), and Acidobacteria (1.1%). The most dominant families included the Methanobacteriaceae (21.8%) in Euryarchaeota, Lachnospiraceae (11.5%), Ruminococcaceae (7.5%), Veillonellaceae (4.9%), Mogibacteriaceae (2.4%), and Peptococcaceae (1.4%) in the Firmicutes, Spirochaetaceae (5.7%) in the Spirochaetes, Bacteroidaceae (3.7%) and Porphyromonadaceae (1.3%) in Bacteroidetes, Cellulomonadaceae (5.8%) in the Acidobacteria, and Desulfovibrionaceae (3.5%) in the Deltaproteobacteria.

No dominant phyla differed across study sampling locations ($P \geq 0.10$). Four dominant phyla differed between heartwood and sapwood tissues. Euryarcheota was 161% greater in heartwood tissue ($34.3 \pm 4.5\%$) compared to sapwood tissue ($13.2 \pm 4.6\%$; $F_{1,25} = 14.1$, $P = 0.001$; Fig. 2) primarily due to OTUs in the genus *Methanobacterium*. In addition, Firmicutes ($F_{1,25} = 7.50$, $P = 0.01$), Acidobacteria ($F_{1,25} = 5.62$, $P = 0.03$), and Deltaproteobacteria ($F_{1,25} = 11.95$, $P = 0.002$) were more abundant in sapwood tissue compared to heartwood. Specifically, Firmicutes was 42% greater ($46.1 \pm 5.9\%$), Deltaproteobacteria was 309% greater ($6.9 \pm 2.0\%$), and Acidobacteria was 546% greater ($2.0 \pm 1.0\%$) in sapwood than heartwood (Firmicutes: 32.6 ± 3.2-%; Acidobacteria: $0.3 \pm 0.1\%$; Deltaproteobacteria: $1.7 \pm 0.5\%$; Fig. S2). Although there were many families which contributed to Firmicutes tissue type differences, the anaerobic family Lachnospiraceae and family Veillonellaceae primarily contributed to the greater abundance in sapwood (Fig. S2). Notably, the genera *Sporomusa*, *Clostridium*, and *Anaerovorax* (the latter two in the Clostridiaceae and Mogibacteriaceae families, respectively) were more abundant in sapwood (Fig. S2). The sulfate-reducing genus, *Desulfovibrio*, from the Deltaproteobacteria contributed to an increased abundance in sapwood tissue, whereas no OTUs classified down to family or genus contributed to the Acidobacteria increases in sapwood.

Multiple phylogenetic groups varied in association with tree physical characteristics. In both heartwood ($T = -3.54$, $P = 0.005$, Adj. $R^2 = 0.49$) and sapwood ($T = -2.60$, $P = 0.03$, Adj. $R^2 = 0.38$) tissues, Methanobacteriaceae abundance was negatively correlated with DBH indicating this group was more abundant in *Populus deltoides* with smaller diameters (Fig. 2b). Other phyla level groups correlated with different tree characteristics depending on tissue type (Fig. S3). Within heartwood tissue, Firmicutes abundance did not correlate with any measurement ($P = 0.24$), but correlated negatively with moisture content in sapwood ($T = -2.67$, $P = 0.02$, Adj. $R^2 = 0.39$). Bacteroidetes correlated negatively with pH ($T = -3.30$, $P = 0.007$, Adj. $R^2 = 0.45$), but was correlated positively with DBH in sapwood tissue ($T = 2.31$, $P = 0.04$, Adj. $R^2 = 0.26$). Within heartwood tissues only, Chloroflexi correlated positively with pH ($T = 2.42$, $P = 0.04$; Adj. $R^2 = 0.55$). Actinobacteria were correlated negatively with DBH ($T = -3.63$, $P = 0.004$, Adj. $R^2 = 0.50$) whereas Spirochaetes were correlated positively with DBH ($T = 3.98$, $P = 0.003$, Adj. $R^2 = 0.66$). Lastly, Alphaproteobacteria abundance correlated negatively with wood moisture content ($T = -3.04$, $P = 0.01$, Adj. $R^2 = 0.41$).

Similar to microbial group abundance differences, OTU-level community composition also shifted between tissue types. Unweighted and weighted Unifrac distance-based community composition were both influenced by tissue type only ($P = 0.001$, $R^2 \geq 0.16$; Table S2). Bray–Curtis distance-based community composition was most influenced by study location ($P = 0.01$, $R^2 = 0.18$) and secondarily by tissue type ($P = 0.003$, $R^2 = 0.20$; S2). This suggests inclusion of phylogenetic relatedness within communities was an important factor in determining differences between heartwood and sapwood tissues for overall OTU composition (Fig. 3). Consistent with increased methane production, predicted mcrA abundance from PICRUSt analyses were $2.6\times$ greater in heartwood tissue relative to sapwood tissue ($T = 4.62$, $P < 0.01$, Fig. S4), along with both methanogenesis and nitrogen transformation pathways in general (Figs S5, S6).
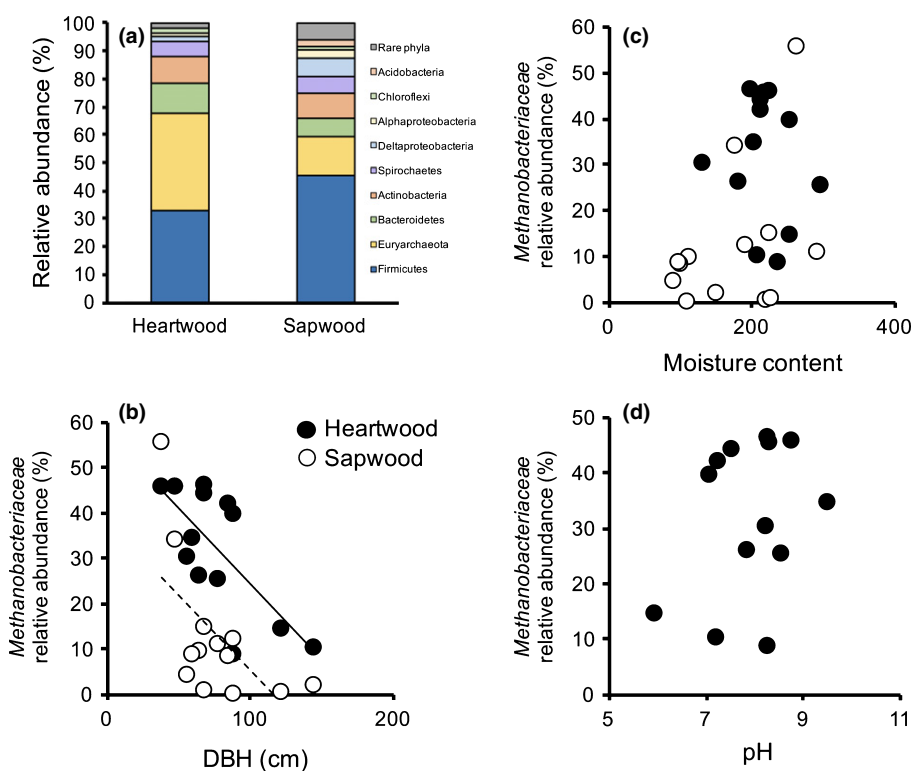

Fig. 2 Mean relative abundance of dominant (> 1.0%) bacterial and archaeal phyla, or subphyla for Proteobacteria, across tissue types in *Populus deltoides* trees (heartwood vs sapwood) (a), the relative abundance of dominant methanogen family, *Methanobacteriacae*, was inversely correlated with diameter at breast height (DBH) (b), but did not correlate with moisture content (c), or pH (d). Heartwood tissue is denoted by black circles and sapwood tissue is denoted by white circles in (b–d). Bolded linear regression lines correspond with black points and dashed regression lines correspond with white points.

Discussion

Biogeochemical gas-flux studies increasingly indicate the importance of wood-associated methane emissions, yet there has been a significant gap in the literature describing the microbial ecology of these systems. Our analysis confirms the prevalence of methanogens and other potentially fermentative organisms living in Eastern Cottonwood woody tissue environments. This study thus supports the concept of living trees acting as a methane source and points to the microbiomes within woody tissues as a significant contributor (Covey *et al.*, 2012; Wang *et al.*, 2016, 2017; Pitz & Megonigal, 2017; Pitz *et al.*, 2018). Consistent with this conclusion, previous work at our study site found < 1% Euryarchaeota in these surface soil communities (Gottel *et al.*, 2011; Shakya *et al.*, 2013). Within woody tissues, the most dominant Euryarcheota OTU was classified as *Methanobacterium* and reached > 40% relative abundance in many samples. OTUs identified as members of the *Methanobrevibacter* were only identified in three samples reaching a maximum of 0.7% relative abundance before rarefying. Both of these sister genera are members of the Methanobacteriaceae family and isolates that have been tested physiologically are known for their relatively high tolerance of oxygen. However, the *Methanobacterium* dominance in our study contrasts with the only other known isolate-based work in *Populus deltoides* (Zeikus & Henning, 1975), where only *Methanobrevibacter* were isolated (and thus presumably dominant) rather than *Methanobacterium* spp. Contrary to our expectation, while OTUs traceable to families known to contain methanotrophs (Knief, 2015) including the Methylobacteriaceae, Methylocystaceae, Beijerinckiaceae (Alpha-Proteobacteria) and the Methylococcaceae (Gamma-Proteobacteria) were present, they were exceedingly rare in both the heartwood and sapwood (0.04% vs 0.1% respectively when these families are totaled together). It is possible that more enriched sublayers may exist in the outermost portions of the sapwood or in the cambium, phloem, or bark that our sampling scheme would not have identified.

Contrary to our expectation, overall DBH was inversely correlated with methanogen abundance in our study (Fig. 2). Wang *et al.* (2017) found positive correlations between the ratio of heartwood diameter to stem diameter and methane stem concentrations and efflux, but no relationship was reported with overall diameter. We assumed that trees of large diameter would be more likely to limit diffusion of oxygen into the heartwood, thereby favoring anaerobic and methanogenic organisms. Further work using more quantitative assessments of methanogen abundance such as quantitative polymerase chain reaction (QPCR) approaches should be used in the future to investigate these relationships, as the community wide relative abundance measures used here do not exclude absolute increases in overall methanogen population size. In our analysis, neither pH or moisture content added significantly to the relationship with DBH and the relative abundance of known methanogenic taxa in stepwise regressions. Others have found that water content of heartwood tissue was the best predictor of methane flux across multiple plant species (Machacova *et al.*, 2016; Wang *et al.*, 2017), however this was not a strong predictor of methanogen relative abundance in our analyses. It is possible that within trees characterized by wetwood such as *Populus deltoides*, other factors

may become more important than water content above a certain moisture threshold. DBH was also inversely correlated with heartwood pH, in that larger trees tended to be more acidic ($R^2 = 0.47$). Although the dominant OTU in our study remains uncharacterized, most *Methanobacteria* spp. have neutral or slightly
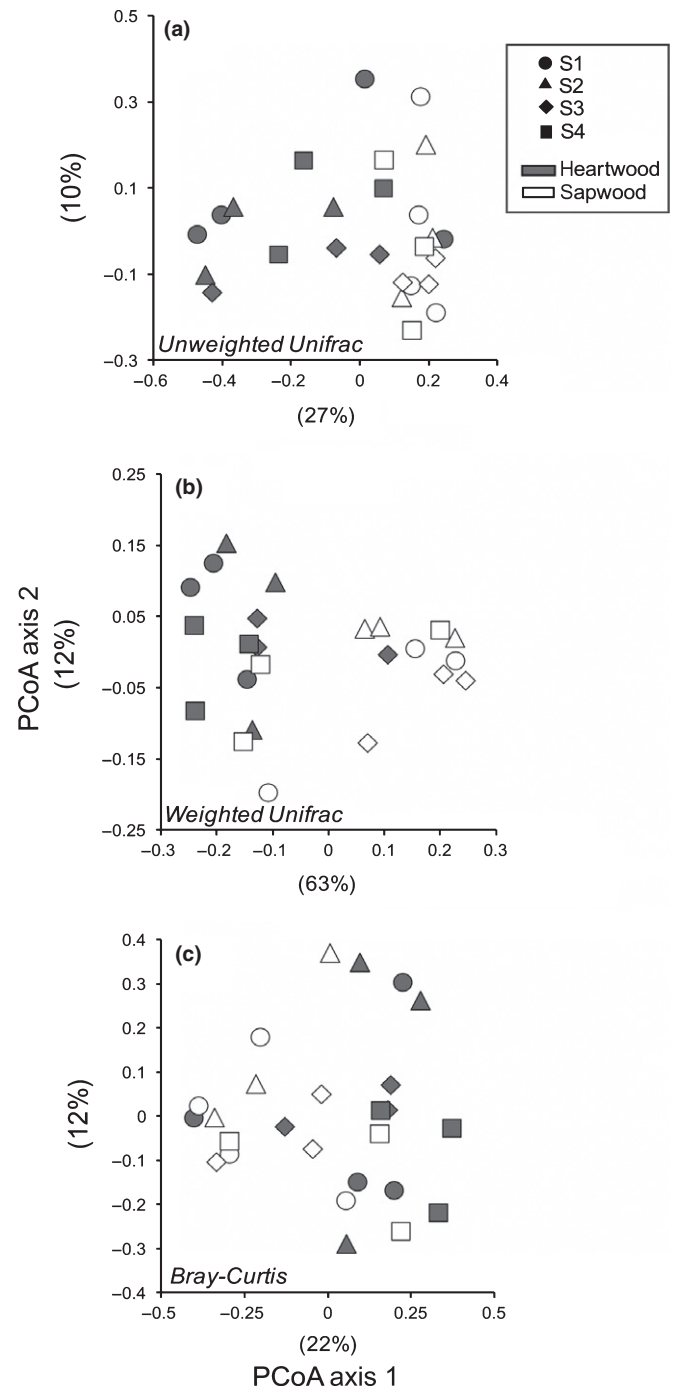

Fig. 3 Principal coordinates analysis (PCoA) with (a) unweighted Unifrac distance, (b) weighted Unifrac distance and (c) Bray–Curtis distance for 16S rRNA gene-based communities. Different symbols (S1–S4) represent study locations 1 through 4; gray symbols, *Populus deltoides* heartwood samples; white symbols, sapwood samples. *Populus deltoides* tissue type influenced community composition in all case, but the significance of study location varied with distance matrix evaluated (see Supporting Information Table S2).

basic pH optima (Oren, 2014), therefore DBH may have merely co-varied with other environmental variables which exerted a more direct influence on methanogenic archaeal abundances. While the trees sampled in our study were mature and represented a fairly large diameter range (range 37.5–144 cm), more extensive studies will be required to understand how well this relationship holds for other tree species, and what direct anatomical features and environmental conditions drive methanogenic community development.

Finally, as these are living systems, the relationship between methane flux and tree features is not likely to be static. Indeed, it was recently demonstrated that methane efflux maxima occurred in diurnal cycles (Pitz & Megonigal, 2017), suggesting a relationship with tree water use or sap flow conditions. Such dynamic interactions will be interesting to address in future studies that should ideally directly couple measures of tree physiology, gas-flux patterns, and changes in microbial community activity using RNA expression-based approaches. Such approaches would inevitably be of interest for parsing the mechanisms of these interactions, and could be essential for better predictions of methane dynamics in our changing environment.

Acknowledgements

Author contributions

D.Z.Y. and C.W.S. designed the study and conducted the field sampling and data collection; D.Z.Y. and Z.K.Y. collected the laboratory data; A.M.V. conducted the data analyses; D.Z.Y., A.M.V., M.A.C. and C.W.S. wrote the manuscript; D.Z.Y., A.M.V. and C.W.S. contributed equally to this work.

References

Anderson MJ. 2001. A new method for non-parametric multivariate analysis of variance. *Austral Ecology* **26**: 32–46.

Balch WE, Fox GE, Magrum LJ, Woese CR, Wolfe RS. 1979. Methanogens – re-evaluation of a unique biological group. *Microbiological Reviews* **43**: 260–296.

Caporaso JG, Kuczynski J, Stombaugh J, Bittinger K, Bushman FD, Costello EK, Fierer N, Pena AG, Goodrich JK, Gordon JI et al. 2010. QIIME allows analysis of high-throughput community sequencing data. *Nature Methods* **7**: 335–336.

Covey KR, Wood SA, Warren RJ II, Lee X, Bradford MA. 2012. Elevated methane concentrations in trees of an upland forest. *Geophysical Research Letters* **39**: 15.

Cregger MA, Veach AM, Yang ZK, Crouch MJ, Vilgalys R, Tuskan GA, Schadt CW. 2018. The *Populus* holobiont: dissecting the effects of plant niches and genotype on the microbiome. *Microbiome* **6**: 31.

Doty SL, Dosher MR, Singleton GL, Moore AL, Van Aken B, Stettler RF, Strand SE, Gordon MP. 2005. Identification of an endophytic *Rhizobium* in stems of *Populus*. *Symbiosis* **39**: 27–35.

Doty SL, Oakley B, Xin G, Kang JW, Singleton G, Khan Z, Vajzovic A, Staley JT. 2009. Diazotrophic endophytes of native black cottonwood and willow. *Symbiosis* **47**: 23–33.

Gottel NR, Castro HF, Kerley M, Yang Z, Pelletier DA, Podar M, Karpinets T, Uberbacher E, Tuskan GA, Vilgalys R et al. 2011. Distinct microbial communities within the endosphere and rhizosphere of *Populus deltoides* roots across contrasting soil types. *Applied and Environment Microbiology* **77**: 5934–5944.

Haas BJ, Gevers D, Earl AM, Feldgarden M, Ward DV, Giannoukos G, Ciulla D, Tabbaa D, Highlander SK, Sodergren E et al. 2011. Chimeric 16S rRNA sequence formation and detection in Sanger and 454-pyrosequenced PCR amplicons. *Genome Research* **21**: 494–504.

Kiener A, Leisinger T. 1983. Oxygen sensitivity of methanogenic bacteria. *Systematic and Applied Microbiology* **4**: 305–312.

Knief C. 2015. Diversity and habitat preferences of cultivated and uncultivated aerobic methanotrophic bacteria evaluated based on pmoA as molecular marker. *Frontiers in Microbiology* **6**: 1346.

Langille MGI, Zaneveld J, Caporaso JG, McDonald D, Knights D, Reyes JA, Clemente JC, Burkepile DE, Thurber RLV, Knight R et al. 2013. Predictive functional profiling of microbial communities using 16S rRNA marker gene sequences. *Nature Biotechnology* **31**: 814–821.

Lozupone C, Hamady M, Knight R. 2006. UniFrac–an online tool for comparing microbial community diversity in a phylogenetic context. *BMC Bioinformatics* **7**: 371.

Lundberg DS, Yourstone S, Mieczkowski P, Jones CD, Dangl JL. 2013. Practical innovations for high-throughput amplicon sequencing. *Nature Methods* **10**: 999–1002.

Machacova K, Back J, Vanhatalo A, Halmeenmaki E, Kolari P, Mammarella I, Pumpanen J, Acosta M, Urban O, Pihlatie M. 2016. *Pinus sylvestris* as a missing source of nitrous oxide and methane in boreal forest. *Scientific Reports* **6**: 23410.

Maier M, Machacova K, Lang F, Svobodova K, Urban O. 2018. Combining soil and tree-stem flux measurements and soil gas profiles to understand CH_4 pathways in *Fagus sylvatica* forests. *Journal of Plant Nutrition and Soil Science* **181**: 31–35.

Martin MJ. 2011. Cutadapt removes adapter sequences from high-throughput sequencing reads. *EMBnet Journal* **17**: 10–12.

Oksanen J, Blanchet FG, Kindt R, Legendre P, Minchin PR, O'hara RB, Simpson GL, Solymos P, Stevens MHH, Wagner H. 2015. vegan: community ecology package. R package version 2.2–1.

Oren A. 2014. The family methanobacteriaceae. In: Delong EF, Lory S, Rosenberg E, Stackebrandt E, Thompson FL, eds. *The Prokaryotes*. Heidelburg, Germany: Springer, 165–193.

Pangala SR, Enrich-Prast A, Basso LS, Peixoto RB, Bastviken D, Hornibrook ERC, Gatti LV, Marotta H, Calazans LSB, Sakuragui CM et al. 2017. Large emissions from floodplain trees close the Amazon methane budget. *Nature* **552**: 230–234.

Pangala SR, Gowing DJ, Hornibrook ER, Gauci V. 2014. Controls on methane emissions from *Alnus glutinosa* saplings. *New Phytologist* **201**: 887–896.

Pangala SR, Hornibrook ER, Gowing DJ, Gauci V. 2015. The contribution of trees to ecosystem methane emissions in a temperate forested wetland. *Global Change Biology* **21**: 2642–2654.

Pangala SR, Moore S, Hornibrook ERC, Gauci V. 2013. Trees are major conduits for methane egress from tropical forested wetlands. *New Phytologist* **197**: 524–531.

Pitz S, Megonigal JP. 2017. Temperate forest methane sink diminished by tree emissions. *New Phytologist* **214**: 1432–1439.

Pitz SL, Megonigal JP, Chang C-H, Szlavecz K. 2018. Methane fluxes from tree stems and soils along a habitat gradient. *Biogeochemistry* **137**: 307–320.

Roberts DW. 2016. *labdsv: Ordination and multivariate analysis for ecology: Version 1.8.* https://CRAN.R-project.org/package=labdsv

Saunois M, Bousquet P, Poulter B, Peregon A, Ciais P, Canadell JG, Dlugokencky EJ, Etiope G, Bastviken D, Houweling S, et al. 2016. The global methane budget 2000-2012. *Earth System Science Data* **8**: 697–751.

Schink B, Thompson TE, Zeikus JG. 1982. Characterization of *Propionispira arboris* gen. nov. sp. nov., a nitrogen-fixing anaerobe common to wetwoods of living trees. *Journal of General Microbiology* **128**: 2771–2779.

Schink B, Ward J, Zeikus J. 1981a. Microbiology of wetwood – importance of pectin degradation and Clostridium species in living trees. *Applied and Environmental Microbiology* **42**: 526–532.

Schink B, Ward J, Zeikus J. 1981b. Microbiology of wetwood – role of anaerobic bacterial populations in living trees. *Journal of General Microbiology* **123**: 313–322.

Seedorf H, Dreisbach A, Hedderich R, Shima S, Thauer RK. 2004. F420H2 oxidase (FprA) from *Methanobrevibacter arboriphilus*, a coenzyme F-420-dependent enzyme involved in O-2 detoxification. *Archives of Microbiology* **182**: 126–137.

Seedorf H, Hagemeier CH, Shima S, Thauer RK, Warkentin E, Ermler U. 2007. Structure of coenzyme F420H2 oxidase (FprA), a di-iron flavoprotein from methanogenic Archaea catalyzing the reduction of O_2 to H_2O. *Febs Journal* **274**: 1588–1599.

Shakya M, Gottel N, Castro H, Yang ZK, Gunter L, Labbe J, Muchero W, Bonito G, Vilgalys R, Tuskan G *et al.* 2013. A multifactor analysis of fungal and bacterial community structure in the root microbiome of mature *Populus deltoides* trees. *PLoS ONE* **8**: e76382.

Streichan M, Schink B. 1986. Microbial-populations in wetwood of European white fir (*Abies alba* Mill). *FEMS Microbiology Ecology* **38**: 141–150.

Tholen A, Pester M, Brune A. 2007. Simultaneous methanogenesis and oxygen reduction by *Methanobrevibacter cuticularis* at low oxygen fluxes. *Fems Microbiology Ecology* **62**: 303–312.

Wang ZP, Gu Q, Deng FD, Huang JH, Megonigal JP, Yu Q, Lu XT, Li LH, Chang S, Zhang YH *et al.* 2016. Methane emissions from the trunks of living trees on upland soils. *New Phytologist* **211**: 429–439.

Wang ZP, Han SJ, Li HL, Deng FD, Zheng YH, Liu HF, Han XG. 2017. Methane production explained largely by water content in the heartwood of living trees in upland forests. *Journal of Geophysical Research–Biogeosciences* **122**: 2479–2489.

Ward J, Zeikus J. 1980. Bacteriological, chemical and physical-properties of wetwood in living trees. *Mitteilungen Der Bundesforschungsanstalt Fur Forst-Und Holzwirtschaft* **131**: 133–166.

Warner DL, Villarreal S, McWilliams K, Inamdar S, Vargas R. 2017. Carbon dioxide and methane fluxes from tree stems, coarse woody debris, and soils in an upland temperate forest. *Ecosystems* **20**: 1205–1216.

Warshaw JE, Leschine SB, Canaleparola E. 1985. Anaerobic cellulolytic bacteria from wetwood of living trees. *Applied and Environmental Microbiology* **50**: 807–811.

Xin G, Zhang GY, Kang JW, Staley JT, Doty SL. 2009. A diazotrophic, indole-3-acetic acid-producing endophyte from wild cottonwood. *Biology and Fertility of Soils* **45**: 669–674.

Zeikus J, Henning D. 1975. *Methanobacterium arbophilicum* sp. nov. an obligate anaerobe isolated from wetwood of living trees. *Antonie Van Leeuwenhoek Journal of Microbiology* **41**: 543–552.

Zeikus JG, Ward JC. 1974. Methane formation in living trees – microbial origin. *Science* **184**: 1181–1183.

Supporting Information

Additional Supporting Information may be found online in the Supporting Information section at the end of the article:

Fig. S1 OTU rarefaction analysis across sample types.

Fig. S2 Simper detected OTUs across heartwood and sapwood environments.

Fig. S3 Correlations between bacterial phyla level relative abundance and tree properties.

Fig. S4 Predicted mcrA gene abundance in PICRUSt analyses of sapwood and heartwood.

Fig. S5 Predicted methane metabolism in heartwood samples based on PICRUSt analyses.

Fig. S6 Predicted nitrogen metabolism in heartwood samples based on PICRUSt analysis.

Table S1 Full table of significant OTUs from Simper analysis

Table S2 Full Adonis analysis results for sample location and tissue type

Video S1 Flammable gasses emitted from tree corer.

Video S2 Fluid and bubbling gasses emitted from tree core hole.

Video S3 Fluid streaming from tree corer after core extraction.

Video S4 Pressure being released from surrounding tree corer.

Please note: Wiley Blackwell are not responsible for the content or functionality of any Supporting Information supplied by the authors. Any queries (other than missing material) should be directed to the *New Phytologist* Central Office.